Truncated variants of hyaluronan-binding protein 1 bind hyaluronan and induce identical morphological aberrations in COS-1 cells

Aniruddha SENGUPTA*, Rakesh K. TYAGI† and Kasturi DATTA*†[1]

*Biochemistry Laboratory, School of Environmental Sciences, Jawaharlal Nehru University, New Delhi 110067, India, and †Special Centre for Molecular Medicine, Jawaharlal Nehru University, New Delhi 110067, India

Hyaluronan (HA)-binding protein 1 (HABP1) is multifunctional in nature and exists as a trimer through coiled-coil interaction between α-helices at its N- and C-termini. To investigate the importance of trimeric assemblage and HA-binding ability of HABP1, we generated and overexpressed variants of HABP1 by truncating the α-helices at its termini. Subsequently, these variants were transiently expressed in COS-1 cells to examine the influence of these structural variations on normal cell morphology, as compared with those imparted by HABP1. Substantiating the centrality of coiled-coil interaction for maintaining the trimeric assembly of HABP1, we demonstrate that disruption of trimerization does not alter the affinity of variants towards its ligand HA. Transient expression of HABP1 altered the morphology of COS-1 cells by generating numerous cytoplasmic vacuoles along with disruption of the f-actin network. Interestingly, the truncated variants also imparted identical morphological changes. Characterization of the cytoplasmic vacuoles revealed that most of these vacuoles were autophagic in nature, resembling those generated under stress conditions. The identical morphological changes manifested in COS-1 cells on transient expression of HABP1 or its variants is attributed to their comparable HA-binding ability, which in concert with endogenous HABP1, may deplete the cellular HA pool. Such quenching of HA below a threshold level in the cellular milieu could generate a stress condition, manifested through cytoplasmic vacuoles and a disassembly of the f-actin network.

Key words: autophagy, hyaluronan-binding protein 1 (HABP1), transient expression, truncated variant, vacuole.

INTRODUCTION

Hyaluronan (HA), a high-molecular-mass glycosaminoglycan, is a principal component of the extracellular matrix of higher animals. Other than its role in maintaining the matrix structure, HA is involved in diverse cellular activities such as cellular transformation and proliferation [1], cell locomotion [2], immune reactions [3] and developmental processes [4]. HA interacts with many different proteins collectively called 'hyaladherins', which influence these biological activities [5]. Some of these hyaladherins are involved in cell–cell or cell–matrix interactions. One such important hyaladherin, first purified from rat liver, is a 68-kDa sialic acid containing glycoprotein termed HABP1 (HA-binding protein 1), having a pI of 4.2 [6]. This cell-surface localized protein [7] has a role in cellular functions similar to cell adhesion and tumour invasion [8], sperm maturity and motility [9,10]. The role of HABP1 in HA-mediated cellular signalling with an increase in the formation of inositol 1,4,5-trisphosphate and phospholipase C-γ combined with enhanced phosphorylation of HABP1 in HA-supplemented cells has already been demonstrated [11]. This protein has been implicated as a substrate for mitogen-activated protein kinase and its differential localization pattern under mitogenic stimulation has been shown in normal and transformed fibroblast cells [12]. The cDNA encoding HABP1 from human fibroblast has been cloned, overexpressed in bacteria and characterized [13].

Sequence analysis and biochemical studies have identified numerous homologous or identical genes for HABP1 in eukaryotic species, ranging from fungi to mammals. The identical genes include p32, a protein co-purified with human splicing factor associated protein (SF2) [14] and gC1qR, receptor for the globular head of the complement subcomponent C1q [15]. Its homology was observed with Mam33p, a mitochondrial matrix protein associated with oxidative phosphorylation in *Saccharomyces cerevisiae* [16] and YL2, an HIV-Rev binding murine homologue [17]. Apart from its ability to bind HA, HABP1 interacts with numerous cellular proteins including transcription factor II B [18], the lamin B receptor [19], vitronectin [20], high-molecular-mass kininogen and factor XII [21]. In addition to cellular proteins, HABP1 also interacts with numerous pathogenic proteins [22–26], indicative of its possible role under conditions of pathogenic stress.

The crystal structure shows it to be a doughnut-shaped homotrimer, with a unique non-crystallographic 3-fold axis of symmetry [27]. Each monomer has seven consecutive β-strands, forming a highly twisted antiparallel β-sheet. The β-strands are flanked by one N-terminal (α-A) and two C-terminal (α-B and α-C) α-helices, where the N-terminal helix (α-A) forms an antiparallel coiled-coil with the C-terminal helix (α-C) of the adjacent subunit, an interaction responsible for the homotrimerization of HABP1. Recent studies have reported the formation of a cysteine-mediated dimer of trimers for HABP1 [28]. Interestingly, the cDNA sequence reveals the presence of a single cysteine residue in each protomer in the polypeptide chain of HABP1 [13]. This oligomerization has functional implications, since the compact structure appears to have higher affinity for HA [29]. Although the binding of HABP1 to HA is reported to occur under oligomeric conditions, interactions of HABP1 with C1q and viral proteins

Abbreviations used: AP, alkaline phosphatase; DIG, digoxigenin; GFP, green fluorescent protein; HA, hyaluronan; HABP1, HA-binding protein 1; MDC, monodansylcadaverine; PCD, programmed cell death.

[1] To whom correspondence should be addressed (e-mail kdatta@mail.jnu.ac.in).

Table 1 Primers used for generating the truncated variants of HABP1

The sequence underlined represents the restriction sites. The combinations of primers used for either amplifying the cDNA or generating the truncated variants of HABP1 are mentioned in the Materials and methods section.

Primer name	Sequence	Position	Restriction site
S1	5′-ggagatatacatatgcacaccgac-3′	Forward	*Nde*I
S2	5′-gcagccggatcctgtaaactc-3′	Reverse	*Bam*HI
S12	5′-ccctccctcatatgtctgga-3′	Forward	*Nde*I
S20	5′-ccccgatatctactcctggtgctccagggc-3′	Reverse	*Eco*RV

have been shown to occur under monomeric conditions as well [15,22–26].

To investigate the importance of trimeric assemblage and HA binding, we generated variants of HABP1 by truncating the α-helices at its N- and C-termini. These PCR-cloned variants were expressed in *Escherichia coli* and analysed for their HA-binding ability. After *in vitro* analysis, we transiently expressed the truncated variants in COS-1 cells and compared the deviations in cellular morphology from those incurred by HABP1.

MATERIALS AND METHODS

Generation of N- and C-terminal truncated variants

HABP1 cDNA was cloned under the *Nde*I and *Bam*HI restriction sites of pET-30b (Novagen) and designated as pET.AS.HABP1. DNA segments for the truncated variants were generated by PCR with pET.AS.HABP1 serving as the template. The forward primers used in the present study had the *Nde*I site, whereas the reverse primer for the N-terminal deleted fragment had a *Bam*HI site and that for the C-terminal deleted fragment had an *Eco*RV site. The primers selected for the study are shown in Table 1. The S1 and S20 primers were used to generate the C-terminal truncated fragment, whereas S12 and S2 primers were used for the N-terminal truncated fragment. PCR was performed using AmpliTaq™ DNA polymerase (PerkinElmer, Norwalk, CT, U.S.A.) according to the following procedure. For a 50 μl reaction, 40 ng of template, 0.15 μM of each primer and 0.25 mM of each dNTP were used. The samples were incubated in a thermal cycler (MJ Research, Waltham, MA, U.S.A.) at 94 °C for 5 min and then kept for 30 cycles of amplification. Each cycle included 45 s denaturation (94 °C), 60 s annealing (55 °C) and 90 s chain elongation (72 °C). After 30 cycles, the reaction was extended for an additional 5 min at 72 °C. The N- and the C-terminal truncated fragments (900 and 600 bp respectively) were purified using Wizard™ SV PCR-purification kit (Promega, Madison, WI, U.S.A.). The N-terminal truncated fragment was digested with *Nde*I and *Bam*HI (New England Biolabs, Beverly, MA, U.S.A.) and cloned at the *Nde*I–*Bam*HI restriction sites of pET-30b and was designated as pET.AS.ΔN.HABP1. The C-terminal truncated fragment was digested with *Nde*I and *Eco*RV and cloned at the *Nde*I–*Eco*RV restriction sites of pET-30b and was designated as pET.AS.ΔC.HABP1.

Confirmation of the clones

The cloning junction and the presence of both the variants were confirmed by restriction digestion and Southern hybridization [30]. The probe used for Southern hybridization was labelled with DIG™ (digoxigenin). In short, a PCR was performed using AmpliTaq™ DNA polymerase, according to the following procedure. For a 25 μl reaction, 20 ng of template, 0.15 μM each of S1 and S20 primers, 0.2 mM dATP, dCTP, dGTP and 0.15 mM dTTP along with 1 μl of DIG–UTP mixed nucleotide (Roche Biochemicals, Basel, Switzerland) were used. The PCR cycles were performed as described previously. The probes were analysed for the amount of DIG incorporated using standard DIG-labelled DNA supplied by the manufacturer.

Expression and purification of the recombinant proteins

HABP1 and its variants were overexpressed in *E. coli* strain BL21(DE3) and purified by ion-exchange chromatography. A single *E. coli* colony was inoculated in 10 ml of Luria–Bertani medium containing 30 μg/ml kanamycin and grown at 37 °C for 9–12 h. Approx. 1 % of the cells were inoculated into 100 ml of Luria–Bertani medium containing 30 μg/ml kanamycin and grown at 37 °C to $A_{600} \sim 0.6$. Protein expression was induced with 1 mM isopropyl β-D-thiogalactoside. After induction, cells were grown at 37 °C for 3 h and collected by centrifugation. The bacterial pellet was suspended in 10 ml of buffer A [20 mM Hepes/1 mM EGTA/1 mM EDTA/5 % (v/v) glycerol, pH 7.5] and disrupted by sonication, until it was optically transparent. The cell extract was centrifuged at 10000 ***g*** for 30 min at 4 °C to remove debris. The supernatant was subjected to 30–90 % ammonium sulphate fractionation at 4 °C, maintaining the pH between 7.5 and 7.8. The ammonium sulphate precipitate was resuspended in buffer A and subjected to SDS/PAGE analysis for optimal percentage of ammonium sulphate required for the precipitation of the desired protein. The fractions thus obtained were pooled and dialysed against 1 litre of buffer A for 16 h. The dialysed sample was centrifuged at 10000 ***g*** at 4 °C for 30 min to remove any particulate matter and then loaded on to Mono-Q™ column HR16 (Amersham Biosciences, Uppsala, Sweden), pre-equilibrated with buffer A. After washing the column with buffer A, the protein was eluted with 0–1 M sodium chloride gradient, using buffer B (20 mM Hepes/1 mM EGTA/1 mM EDTA/5 % glycerol/1 M NaCl, pH 7.5). The peak fractions obtained were analysed on SDS/PAGE and stained with Coomassie Brilliant Blue. Fractions containing the protein of interest were pooled, desalted and concentrated.

Immunoblot analysis

The purified proteins were separated on a 12.5 % SDS/polyacrylamide gel under reducing conditions and transferred on to a nitrocellulose membrane [31]. The membrane was blocked for 1 h with 3 % (w/v) BSA in PBS and then incubated with polyclonal antibodies against HABP1 for 1 h in PBS containing 1.5 % BSA. After washing the blot for 5 × 5 min with PBS supplemented with 0.05 % Tween 20 (PBST), it was further incubated for 1 h with AP (alkaline phosphatase)-conjugated goat anti-rabbit IgG in 1.5 % BSA/PBS. Bound antibodies were detected using Nitro Blue Tetrazolium/5-bromo-4-chloroindol-3-yl phosphate system (Amersham Biosciences, Little Chalfont, Bucks., U.K.).

Size-exclusion chromatography

To determine the native molecular mass of HABP1, ΔN.HABP1 and ΔC.HABP1 in solution, gel filtration experiments were performed on a Superose6™ analytical-grade gel filtration column interfaced with Pharmacia FPLC system. The column was calibrated with the standard proteins aldolase (158 kDa), BSA (67 kDa), ovalbumin (43 kDa), chymotrypsinogen (25 kDa) and RNase A (13.7 kDa) (Amersham Biosciences). The buffer used in the present study was PBS with 150 mM NaCl to keep the ionic strength constant. The elution speed was kept constant throughout the experiment at 0.3 ml/min.

Table 2 Primers used for cloning HABP1 and the truncated fragments into the mammalian expression vector

The sequence underlined represents the restriction sites.

Primer name	Sequence	Position	Restriction site
Mamm 1	5′-tgtgagcagctgacaattcccctct-3′	Forward	*Pvu*II
Mamm 2	5′-gacggagctagcgctcgaattcgg-3′	Reverse	*Nhe*I

Binding of HABP1 and its variants to immobilized HA

The binding of HABP1 and its variants to immobilized HA was measured in 96-well microtitre plates (Costar, Cambridge, MA, U.S.A.). The wells were coated overnight at 4 °C with 2 mg/ml HA in coating buffer (15 mM sodium carbonate and 34 mM sodium bicarbonate, pH 9.3) and blocked for 2 h in 0.25 % BSA and 0.05 % Tween 20 in PBS [32]. After three washes with PBS, the plates were incubated with the purified proteins for 2 h at room temperature (24 °C). After washing off the unbound proteins, the plates were incubated with polyclonal anti-HABP1 antibodies for 1 h at room temperature. After 5×5 min washes with PBS, the plates were incubated with AP-conjugated goat anti-rabbit IgG for 1 h at room temperature. After the unbound secondary antibody was washed off the plates, the reactions were developed using AP-substrate solution (Sigma 104 phosphate) until the desired colour developed. The A_{405} of each well was recorded using a Bio-Rad microtitre plate reader. For control experiment, immobilized HA was first overlaid with BSA and subsequently treated with the antibodies used in the study.

Cloning of HABP1 and its variants into a mammalian expression vector

The HABP1 cDNA and its variants were cloned in the mammalian expression vector pBI-EGFP (ClonTech). The fragments were amplified through PCR using Vent™ DNA polymerase (New England Biolabs) from clones generated in pET-30b and a blunt-end cloning was made at the *Pvu*II restriction site of pBI-EGFP. The primers used in the present study are shown in Table 2.

Cell culture and transfection

The origin-defective SV40-transformed green monkey kidney cells (COS-1), obtained from National Centre for Cell Science (Pune, Maharashtra, India), were grown in Dulbecco's modified Eagle's medium supplemented with 10 % (v/v) foetal calf serum, 100 μg/ml penicillin and 100 μg/ml streptomycin (Invitrogen, Carlsbad, CA, U.S.A.). Transient transfection in COS-1 cells was done with LIPOFECTAMINE™ 2000 (Invitrogen) according to the manufacturer's instructions. For each transfection, 500 ng of kit purified plasmid DNA (Qiagen GmbH, Hilden, Germany) and 6 μl of LIPOFECTAMINE™ 2000 were used. After the transfection period of 8 h, fresh medium was added and the cells were grown for an additional 25–30 h. The transfected cells were then processed for further experiments or imaging.

Analysis of nuclear morphology

For live cells, Hoechst 33 342 was added to the medium of transfected cells 1 h before imaging. For fixed cells, after f-actin detection, the coverslips were washed and stained with Hoechst in PBS for 15 min in the dark. Thereafter the cells were washed with PBS and mounted in PBS/glycerol.

Detection of autophagic vacuoles

Autophagic vacuoles were detected with MDC (monodansylcadaverine) by the method of Biederbick et al. [33]. The transfected cells grown for 30 h were washed with PBS to remove the culture medium. The cells were then incubated with 0.05 mM MDC in PBS at 37 °C for 10 min. After incubation, the cells were washed four times with PBS and immediately analysed by fluorescence microscopy.

Examination of f-actin network

For the detection of f-actin, cells were grown on glass coverslips, fixed with 2 % (w/v) paraformaldehyde and washed with PBS. After permeabilization of the cells with 0.1 % Triton X-100, f-actin was detected by rhodamine–phalloidin (Molecular Probes, Eugene, OR, U.S.A.). Before mounting, the coverslips were counter stained with Hoechst.

Microscopy and image analysis

The transfected cells were either used directly for live cell imaging or analysed after morphological and histochemical detection, using fluorescence microscopy. The fluorescent cells were viewed with an Axioscope microscope (Carl Zeiss, Cologne, Germany) using suitable filter sets, and imaged with the AxioCam camera system coupled with the AxioVision software (Carl Zeiss).

RESULTS AND DISCUSSION

Generation and purification of the truncated variants of HABP1

To study the structure–function relationship of HABP1, the truncated fragments were generated through PCR. Figure 1(A) schematically represents the cDNA sequence of HABP1 cloned in pET-30b, depicting the position of primers used for the generation of the truncated variants. The truncated fragments generated through PCR were 900 and 600 bp for ΔN.HABP1 and ΔC.HABP1 respectively, when compared with 1030 bp for HABP1 (Figure 1B). The fragments were subsequently cloned in the expression vector pET.30b to generate the truncated variant constructs, as described in the Materials and methods section. The cloning junction and the presence of the truncated variants were confirmed by restriction digestion followed by Southern hybridization. The restriction digestion profile generated fragments of 900, 600 and 1030 bp for ΔN.HABP1, ΔC.HABP1 and HABP1 respectively, which could be detected by Southern hybridization using DIG-labelled cDNA probe, thus establishing the proper cloning of the fragments (Figures 1C and 1D). The constructs were subsequently sequenced to establish their authenticity (results not shown).

A diagrammatic representation of the variants and their comparison with HABP1 is shown in Figure 2(A). The proteins were successfully overexpressed in *E. coli* and we have purified the protein (HABP1), the N-terminal truncated variant (ΔN.HABP1) and the C-terminal truncated variant (ΔC.HABP1) using an ion-exchange column on the FPLC. The proteins were purified to >95 % homogeneity, as determined by Coomassie Brilliant Blue staining of SDS/PAGE, where HABP1, ΔN.HABP1 and ΔC.HABP1 correspond to 34, 27 and 32 kDa respectively (Figure 2B). This anomalous migration of HABP1 and its variants could be attributed to the presence of more than average polar amino acid residues on these proteins [28]. The calculated pI values for ΔN.HABP1 and ΔC.HABP1 were 4.05 and 4.21 respectively. The antigenic specificity of the proteins was examined

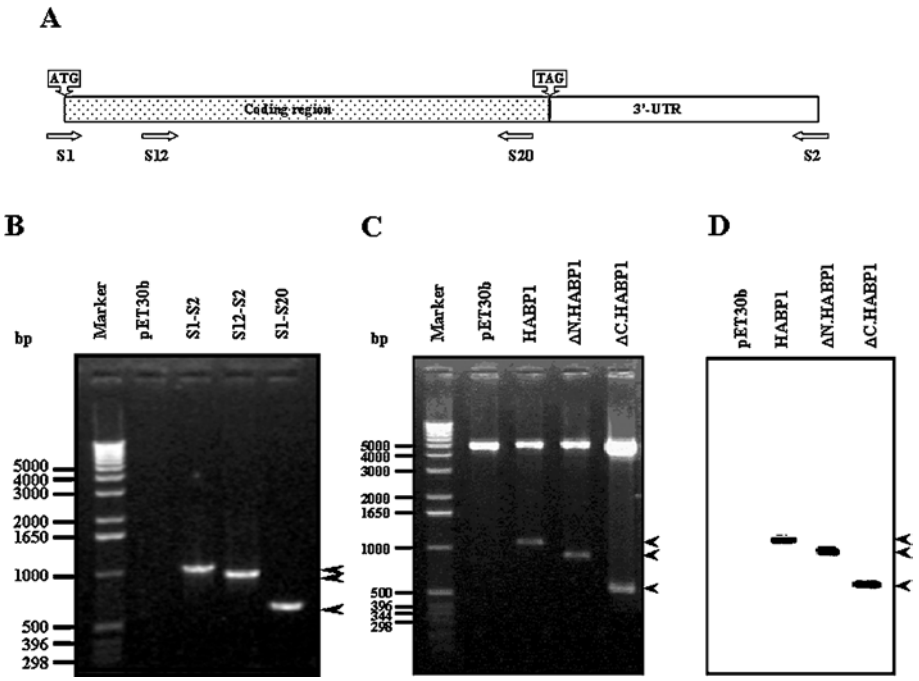

Figure 1 Generation and confirmation of the truncated variants of HABP1

(**A**) A schematic representation of HABP1 variants generated in the present study. The position of primers on the cDNA template is shown, and the first amino acid in the coding region (ATG) and the termination codon (TAG) have been marked in the scheme. (**B**) pET.AS.HABP1 was used as the template for PCR, using the primer combinations mentioned in the Materials and methods section, whereas pET-30b in combination with S1–S2 primers was used as a negative control. The amplified products were analysed on a 1.2 % (w/v) agarose gel alongside 1 kb DNA molecular-mass standards (Invitrogen). The amplified fragments in each lane are marked with an arrow. (**C**) HABP1 and the truncated fragments, cloned in pET-30b, were digested with *Nde*I and *Bam*HI restriction endonucleases and resolved on a 1.5 % agarose gel. The fragment generated from HABP1 was 1030 bp in length, whereas those from ΔN.HABP1 and ΔC.HABP1 were 900 and 600 bp respectively. (**D**) Southern hybridization using DIG-labelled cDNA probe specifically detected the fragments, thus establishing their proper cloning.

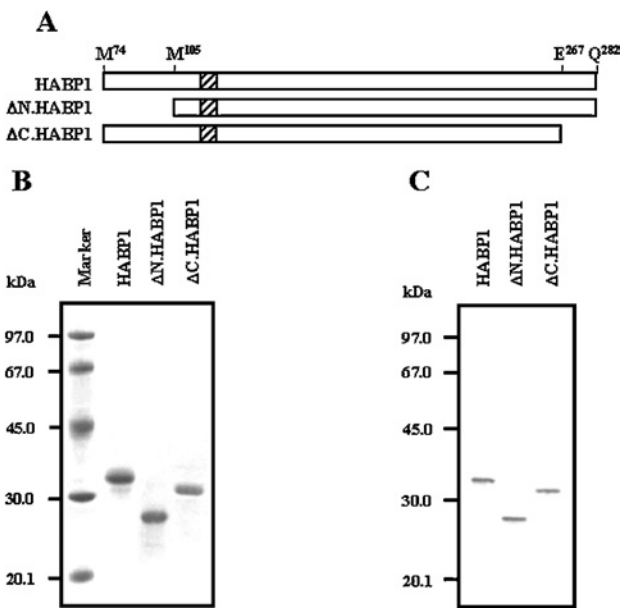

Figure 2 Purification and immunodetection of the truncated proteins

(**A**) HABP1 and its variants are schematically depicted indicating the HA-binding motif (shaded). The amino acids 74–104 of HABP1 have been deleted to generate ΔN.HABP1, whereas amino acids 268–282 have been deleted to generate ΔC.HABP1. In ΔC.HABP1, a stop codon has been introduced after Glu-267. In the recombinant protein, Leu-74 has been replaced with Met-74. (**B**) HABP1, ΔN.HABP1 and ΔC.HABP1 were purified and resolved by SDS/PAGE (12.5 % gel) followed by staining with Coomassie Brilliant Blue to analyse their subunit molecular mass. (**C**) The proteins were transferred on to nitrocellulose membrane and immunodetected by Western blotting using polyclonal anti-HABP1 antibodies.

by immunodetection using anti-HABP1 polyclonal antibodies (Figure 2C), which clearly demonstrated antigenic similarity of the variants to HABP1.

Truncation of terminal helices of HABP1 abolishes oligomerization

Oligomeric states of HABP1 and its variants were examined by size-exclusion chromatography. Standard proteins used for the calibration of the column have been marked 1–5, depicting aldolase, BSA, ovalbumin, chymotrypsinogen and RNase A respectively (Figure 3A). HABP1 exists primarily as a trimer in equilibrium with disulphide-mediated dimer of trimer, exhibiting trimeric and hexameric molecular masses of 68 and 136 kDa under non-reducing gel filtration chromatography. The variants exhibited the presence of monomeric and dimeric forms corresponding to 20 and 40 kDa for ΔN.HABP1 and 22 and 44 kDa for ΔC.HABP1 under non-reducing gel filtration chromatography (Figure 3B). However, under reducing conditions (0.02 % 2-mercaptoethanol), ΔN.HABP1 and ΔC.HABP1 exhibited monomeric species only (Figure 3C), whereas HABP1 exhibits only the trimeric species. These results substantiate that truncation at either N- or C-terminal generates variants, which are incapable of forming a trimer by coiled-coil interaction of the α-helices. It also shows that under normal or physiological conditions, the variants tend to form a disulphide linkage, giving rise to the dimer apart from the monomer, whereas HABP1 exists primarily as trimer and hexamer under such conditions. The two forms, the disulphide-linked dimer as well as the monomer, exist in equilibrium. These observations are consistent with our earlier report of conformational flexibility of HABP1 [29].

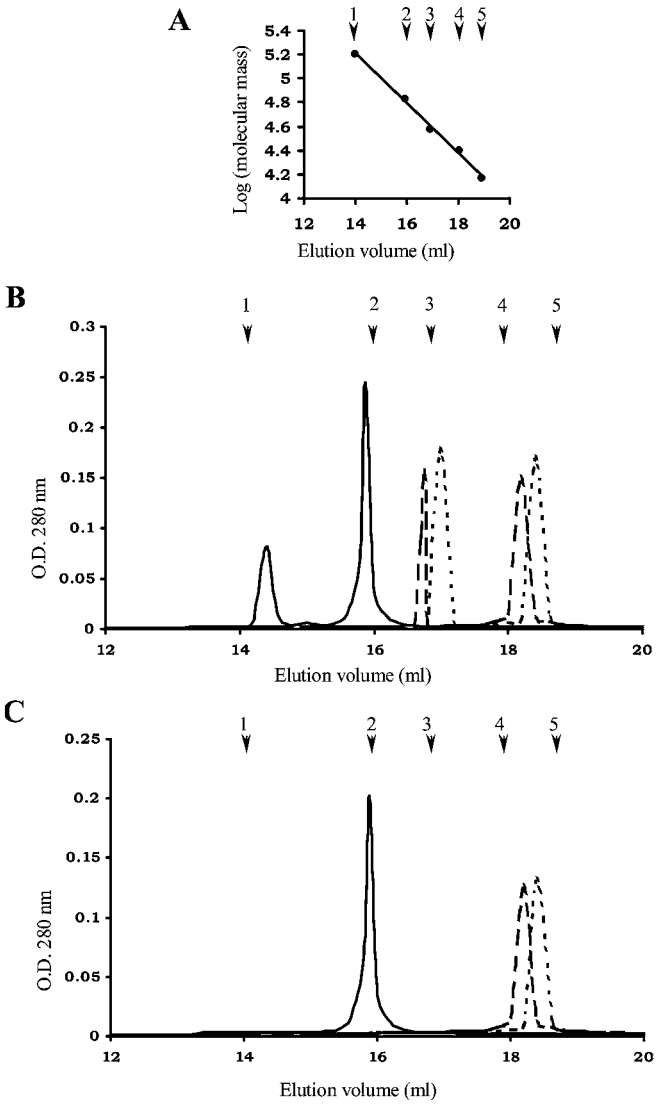

Figure 3 Truncation of terminal helices of HABP1 abolishes oligomerization

(**A**) The elution profile of the column calibration markers, plotted against the logarithm of molecular mass. The calibration markers, aldolase (158 kDa), BSA (67 kDa), ovalbumin (43 kDa), chymotrypsinogen (25 kDa) and RNase A (13.7 kDa) are labelled through 1–5, in the order of decreasing molecular mass and the same labelling is followed throughout. The gel filtration analysis of HABP1 (—), ΔN.HABP1 (- - - -) and ΔC.HABP1 (– – – –) were performed under (**B**) non-reducing conditions and (**C**) reducing conditions (in the presence of 0.2 % 2-mercaptoethanol).

HA-binding ability of the variants is comparable with HABP1

Earlier studies from our laboratory have already shown that HABP1 binds HA under trimeric or hexameric conditions [28]. However, the variants do not possess this trimeric assembly, as evident from the size-exclusion chromatography results (Figure 3). The HA-binding ability of each variant was examined using immobilized HA. ELISA strips coated with HA were overlaid with protein sample and detected using antibodies, as described in the Materials and methods section. Results indicate that both ΔN.HABP1 and ΔC.HABP1 effectively bind to HA (Figure 4) and their binding efficiency is comparable with HABP1. Thus although terminal deletions alter the oligomerization property of the variants, they retain their ability to bind HA. This suggests that although the variants have an altered structure, their HA-binding

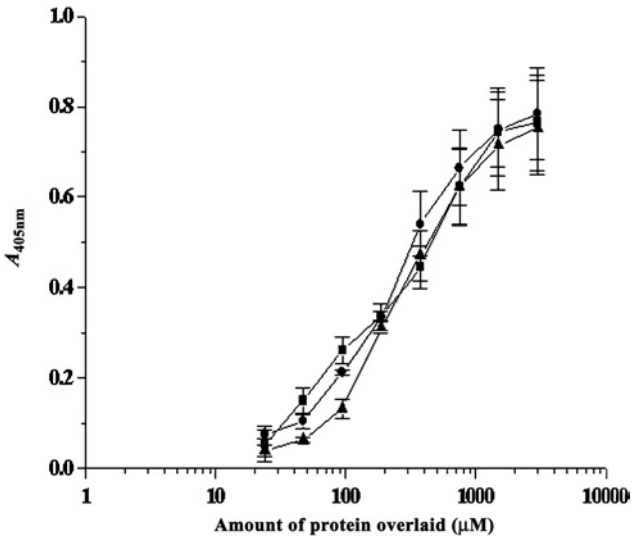

Figure 4 HA-binding ability of the variants is comparable with that of HABP1

Immobilized HA on ELISA plates was used to compare the HA-binding ability of ΔN.HABP1 (■) and ΔC.HABP1 (▲) with that of HABP1 (●). The proteins (in PBS) were overlaid on immobilized HA under non-reducing conditions. The background reading for the control (BSA) has been subtracted from the experimental samples. Results represent the average of duplicate determinations in at least three identical experiments, performed under similar conditions.

motif remains accessible to the solvent, a proposition reflected in their HA-binding ability. This motif remains unaltered in variants and dimerization of the variants may juxtapose each monomer in a manner that allows it to be accessible for binding. From this observation, it appears that the juxtaposition of the HA-binding motif may be a predominant influence for HA binding rather than just the oligomeric structure and compactness of HABP1.

Expression of HABP1 and its variants in COS-1 cells induces identical morphological changes

To compare the morphological and cellular changes imparted by HABP1 and its variants, the cDNA were cloned in the mammalian expression vector pBI-EGFP and expressed in COS-1 cells. The bi-directional vector pBI-EGFP aided us in evaluating the cellular morphology of living cells, as GFP (green fluorescent protein) would distribute uniformly in the cell and divulge visible changes thereof. The constructs were authenticated for their orientation in pBI-EGFP and then transiently expressed in COS-1 cells. The vector pBI-EGFP, expressing GFP, served as control for all comparative analysis. Although no visible change in the shape and size of the cells was evident, the transfected cells exhibited altered morphology, with numerous conspicuous cytoplasmic caveolar-like circular structures resembling vacuoles (Figure 5A). These structures have been henceforth referred to as ‘vacuoles’. The cells were stained with Hoechst for visualizing the nucleus, whereas the presence of GFP facilitated cell-morphology analysis in living cells. These results are in agreement with our earlier reports, where the formation of similar cytoplasmic vacuoles has been shown in a cell lines stably expressing HABP1 [34]. The presence of small vacuoles in cultured cell lines is not an unknown feature; however, owing to an increase in the size and the number of vacuoles after transient expression of the proteins, a statistical analysis ($n = 10$) of each clone was performed. This was done to estimate whether the vacuole formation was an artifact of transfection or a morphological manifestation of cellular changes

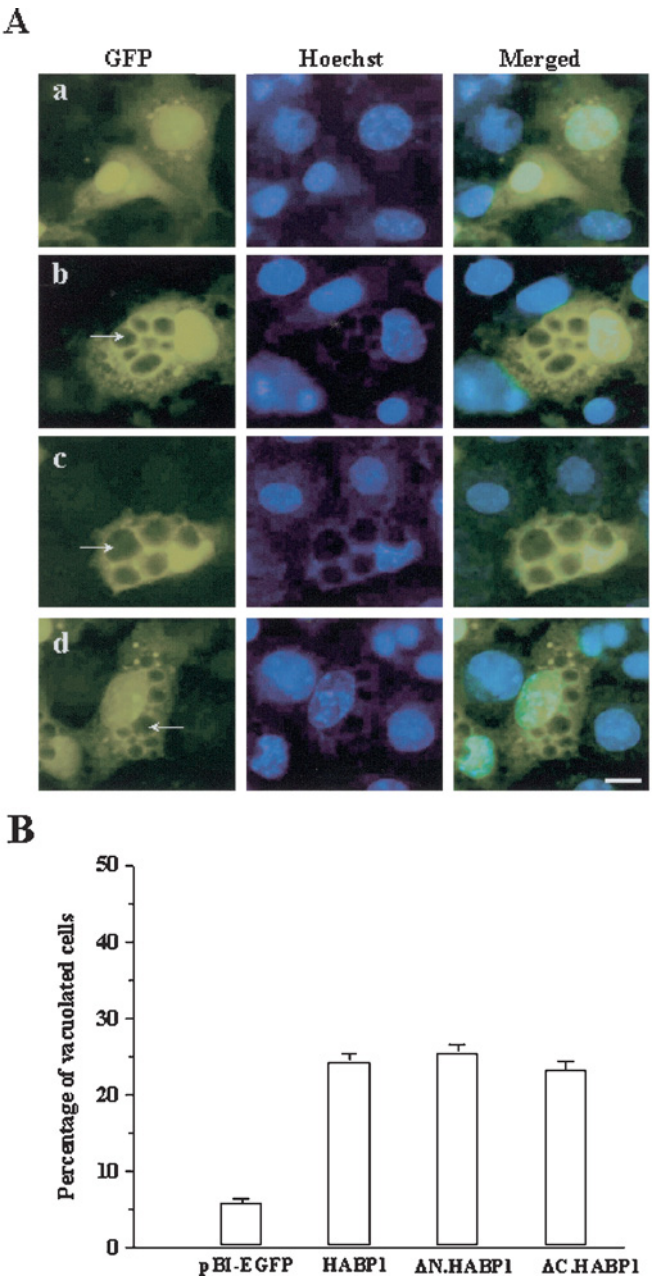

Figure 5 Expression of HABP1 and its variants induce identical morphological changes

(**A**) The COS-1 cells transfected with (**a**) pBI-EGFP showed less vacuole formation when compared with cells transfected with (**b**) HABP1, (**c**) ΔN.HABP1 or (**d**) ΔC.HABP1. The Figure shows representative images for each sample. The first column shows the morphology as depicted by the distribution of GFP, whereas the second column reveals cell nuclei, visualized through Hoechst staining. The third column shows the superimposed images corresponding to GFP and Hoechst merged together. The conspicuous vacuoles have been labelled with an arrow. Scale bar, 10 μm. (**B**) A statistical analysis for the percentage of vacuole-bearing cells in the transfected population, as compared with the vector control. Results represent means $\pm$ S.D. for ten independent experiments for each clone.

due to expression of the proteins. These results revealed a 4-fold increase in the percentage of transfected cells harbouring vacuoles in cells expressing HABP1 or its variants (Figure 5B). However, it needs to be emphasized that vacuole formation was not an inherent manifestation of plasmid transfection or GFP expression, as evident from the percentage of cells exhibiting them.

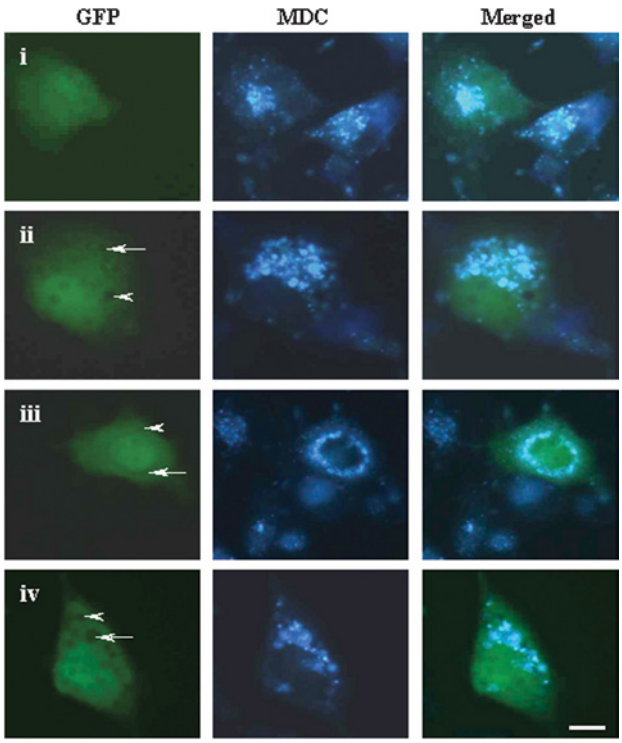

Figure 6 Detection of autophagic vacuoles through MDC in the transfected cells

MDC staining of the conspicuous vacuoles reveal them to be both autophagic (white arrows) and non-autophagic (white arrowheads) in nature. The cells transfected with HABP1 (**ii**), ΔN.HABP1 (**iii**) and ΔC.HABP1 (**iv**) reveal increased autophagic vacuoles, when compared with the vector (**i**). The Figure shows representative images for each sample. The first column shows the morphology of the transfected cells, as depicted by the distribution of GFP, whereas the second column reveals autophagic vacuoles, visualized through MDC staining. The third column shows the superimposed images corresponding to GFP and MDC merged together. Scale bar, 10 μm.

The generation of conspicuous cytoplasmic vacuoles after transient expression of HABP1 or its variants prompted us to characterize their nature. In general, cytoplasmic vacuoles are often autophagic in nature. Transfected cells were stained with MDC as it has been successfully used in determining autophagic vacuole [35]. Results reveal the population of vacuoles to be heterogeneous, being both autophagic and non-autophagic in nature (Figure 6). However, MDC staining reveals that the cells transiently expressing HABP1 or its variants show more prominent autophagic vacuoles, when compared with the vector control, indicating that these autophagic vacuoles were not an outcome of GFP expression but a consequence of expression of HABP1 or it variants. Autophagy has been considered as an adaptive response to nutrient deprivation, stress conditions, tissue-specific biogenesis and a housekeeping mechanism involved in cytoplasmic homoeostasis, as it controls the turnover of peroxisomes, mitochondria and the size of the endoplasmic reticulum [36]. Earlier studies on autophagic vacuoles have established their acidic nature [37,38]. HABP1 and its variants manifest pI of approx. 4; consequently, their acidic nature makes them probable candidates for entry into the vacuoles. Stress conditions often lead to the formation of autophagic vacuoles [35,39] and transient expression of HABP1 or its variants in COS-1 cells might evoke a similar phenomenon, forcing the cells to take up autophagy as an adaptive response. Autophagy is also involved in maintaining a balance between protein synthesis and degradation [40] and is often associated with stress conditions and diseased states, leading

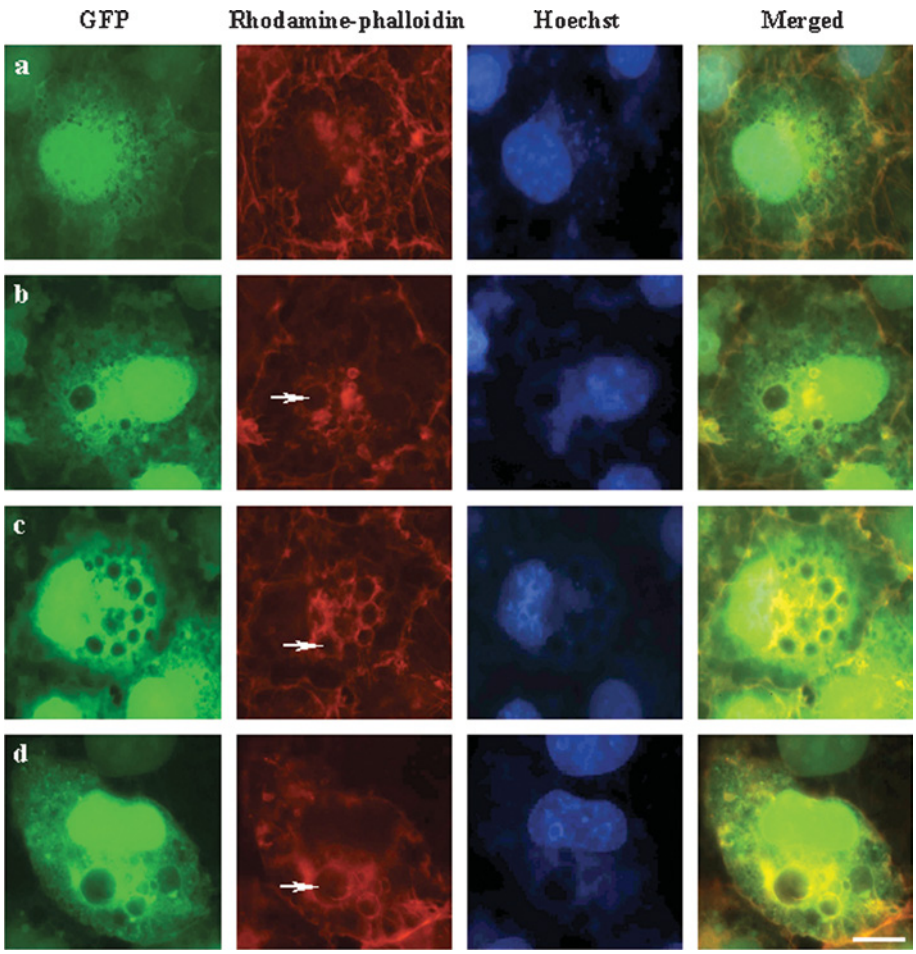

Figure 7 Examination of the f-actin network in the transfected cells

Rhodamine–phalloidin staining of the transfected cells revealed a disassembly of the f-actin network. The cells transfected with HABP1 (**b**), ΔN.HABP1 (**c**) and ΔC.HABP1 (**d**) reveal f-actin aggregation around the nucleus and it appears disassembled, with a distinct disruption at the vacuolar region, when compared with the vector (**a**). The conspicuous vacuoles are marked with an arrow. The Figure shows representative images for each sample. The first column shows the morphology of the transfected cells, as depicted by the distribution of GFP; the second column reveals f-actin network, detected through rhodamine–phalloidin staining; whereas the third column reveals nuclear morphology, visualized through Hoechst staining. The superimposed images corresponding to GFP, rhodamine and Hoechst, merged together, are shown in the third column. Scale bar, 15 μm.

to PCD (programmed cell death) [41]. HABP1 is a constitutive multifunctional protein and its transient expression in cells might interfere with the functioning of endogenous HABP1, altering the cellular homoeostasis and affecting stress conditions, which leads to the generation of vacuoles. The formation of vacuoles might indicate PCD and cells manifesting them may undergo such a process soon thereafter, as already shown by our earlier studies on cell lines stably expressing HABP1 [34].

A cytoskeletal network is an integral feature of all cells, and its disruption often reflects a departure from normal cellular behaviour. Therefore, in supporting experiments, the fate of f-actin was studied to observe any alteration in cytoskeletal network resulting from the transient expression of HABP1 or its variants. As evident from Figure 7, the cells transiently expressing HABP1 or its variants disrupted the f-actin network, a key component of the cytoskeleton. F-actin appeared to aggregate around the nucleus, with a distinct disassembly at the vacuolar region. Cytoskeletal proteins are often associated with PCD and the disruption of the microfilament network or depolymerization of f-actin in cell death has already been shown [42,43]. In accordance with this, our investigation on f-actin in cells transiently expressing HABP1 or its variants indicated a disassembly in the network. Taken together, our observations indicate that the expression of HABP1 or its truncated variants in cultured mammalian cells impart identical morphological changes.

Conclusion

Although earlier studies have established that trimerization of HABP1 is critical for HA binding, the present observations reveal that a juxtaposition of the HA-binding motif may play a dominant role in this phenomenon. We have shown that HABP1 and its variants bind HA with comparable affinity and their expression induces identical cytoplasmic vacuoles and a disruption of f-actin network in cultured mammalian cells. Most of these vacuoles, apparently generated through stress conditions, have been shown to be autophagic in nature. These identical morphological changes imparted by the transient expression of HABP1 or its variants appear to be due to their comparable HA affinity rather than their structural variations. In the light of the present observations, we hypothesize that the overall increase in the level of cellular HABP1 (expressed and endogenous) beyond the housekeeping requirement may deplete the cellular ‘HA pool’ to such a critical extent that it results in the generation of a stress condition

leading to the formation of vacuoles. Therefore, in principle, the orchestration of 'HA pool' by hyaladherins appears to play a key role in regulating the cellular functions of HA.

This Research was supported by grants from the Department of Biotechnology, the Department of Science and Technology, Government of India. A. S. acknowledges the University Grants Commission for the award of a research fellowship.

REFERENCES

1 Laurent, T. C. and Fraser, J. R. (1992) Hyaluronan. FASEB J. **6**, 2397–2404
2 Toole, B. P. (1981) Glycosaminoglycans in morphogenesis. In Cell Biology of the Extracellular Matrix (Hay, E. D., ed.), pp. 259–294, Plenum Press, New York
3 Clarris, B. J. and Fraser, J. R. (1968) On the pericellular zone of some mammalian cells *in vitro*. Exp. Cell Res. **49**, 181–193
4 Knudson, C. B. and Knudson, W. (1993) Hyaluronan binding proteins in development, tissue homeostasis and disease. FASEB J. **7**, 1233–1241
5 Toole, B. P. (1990) Hyaluronan and its binding proteins, the hyaladherins. Curr. Opin. Cell Biol. **2**, 839–844
6 D'Souza, M. and Datta, K. (1985) Evidence for naturally occurring hyaluronic acid binding protein in rat liver. Biochem. Int. **10**, 43–51
7 Gupta, S., Batchu, R. B. and Datta, K. (1991) Purification, partial characterization of rat kidney hyaluronic acid binding protein and its localization on the cell surface. Eur. J. Cell Biol. **56**, 58–67
8 Gupta, S. and Datta, K. (1991) Possible role of hyaluronectin on cell adhesion in rat histiocytoma. Exp. Cell Res. **195**, 386–394
9 Ranganathan, S., Ganguly, A. K. and Datta, K. (1994) Evidence for presence of hyaluronan binding protein on spermatozoa and its possible involvement in sperm function. Mol. Reprod. Dev. **38**, 69–76
10 Ranganathan, S., Bharadwaj, A. and Datta, K. (1995) Hyaluronan mediates sperm motility by enhancing phosphorylation of proteins including hyaluronan binding protein. Cell Mol. Biol. Res. **41**, 467–476
11 Rao, C. M., Deb, T. B., Gupta, S. and Datta, K. (1997) Regulation of cellular phosphorylation of hyaluronan binding protein and its role in the formation of second messenger. Biochim. Biophys. Acta **1336**, 387–393
12 Majumdar, M., Meenakshi, J., Goswami, S. K. and Datta, K. (2002) Hyaluronan binding protein 1 (HABP1)/C1QBP/p32 is an endogenous substrate for MAP kinase and is translocated to the nucleus upon mitogenic stimulation. Biochem. Biophys. Res. Commun. **291**, 829–837
13 Deb, T. B. and Datta, K. (1996) Molecular cloning of human fibroblast hyaluronic acid-binding protein confirms its identity with P-32, a protein co-purified with splicing factor SF2. Hyaluronic acid-binding protein as P-32 protein, co-purified with splicing factor SF2. J. Biol. Chem. **271**, 2206–2212
14 Krainer, A. R., Mayeda, A., Kozak, D. and Binns, G. (1991) Functional expression of cloned human splicing factor SF2: homology to RNA-binding proteins, U1 70K, and *Drosophila* splicing regulators. Cell (Cambridge, Mass.) **66**, 383–394
15 Ghebrehiwet, B., Lim, B. L., Peerschke, E. I., Willis, A. C. and Reid, K. B. (1994) Isolation, cDNA cloning, and overexpression of a 33-kD cell surface glycoprotein that binds to the globular 'heads' of C1q. J. Exp. Med. **179**, 1809–1821
16 Seytter, T., Lottspeich, F., Neupert, W. and Schwarz, E. (1998) Mam33p, an oligomeric, acidic protein in the mitochondrial matrix of *Saccharomyces cerevisiae* is related to the human complement receptor gC1q-R. Yeast **14**, 303–310
17 Luo, Y., Yu, H. and Peterlin, B. M. (1994) Cellular protein modulates effects of human immunodeficiency virus type 1 Rev. J. Virol. **68**, 3850–3856
18 Yu, L., Loewenstein, P. M., Zhang, Z. and Green, M. (1995) *In vitro* interaction of the human immunodeficiency virus type 1 Tat transactivator and the general transcription factor TFIIB with the cellular protein TAP. J. Virol. **69**, 3017–3023
19 Simos, G. and Georgatos, S. D. (1994) The lamin B receptor-associated protein p34 shares sequence homology and antigenic determinants with the splicing factor 2-associated protein p32. FEBS Lett. **346**, 225–228
20 Lim, B. L., Reid, K. B., Ghebrehiwet, B., Peerschke, E. I., Leigh, L. A. and Preissner, K. T. (1996) The binding protein for globular heads of complement C1q, gC1qR. Functional expression and characterization as a novel vitronectin binding factor. J. Biol. Chem. **271**, 26739–26744
21 Lim, B. L., White, R. A., Hummel, G. S., Schwaeble, W., Lynch, N. J., Peerschke, E. I., Reid, K. B. and Ghebrehiwet, B. (1998) Characterization of the murine gene of gC1qBP, a novel cell protein that binds the globular heads of C1q, vitronectin, high molecular weight kininogen and factor XII. Gene **209**, 229–237
22 Matthews, D. A. and Russell, W. C. (1998) Adenovirus core protein V interacts with p32 – a protein which is associated with both the mitochondria and the nucleus. J. Gen. Virol. **79**, 1677–1685
23 Wang, Y., Finan, J. E., Middeldorp, J. M. and Hayward, S. D. (1997) P32/TAP, a cellular protein that interacts with EBNA-1 of Epstein–Barr virus. Virology **236**, 18–29
24 Tange, T. O., Jensen, T. H. and Kjems, J. (1996) *In vitro* interaction between human immunodeficiency virus type 1 Rev protein and splicing factor ASF/SF2-associated protein, p32. J. Biol. Chem. **271**, 10066–10072
25 Yu, L., Zhang, Z., Loewenstein, P. M., Desai, K., Tang, Q., Mao, D., Symington, J. S. and Green, M. (1995) Molecular cloning and characterization of a cellular protein that interacts with the human immunodeficiency virus type 1 Tat transactivator and encodes a strong transcriptional activation domain. J. Virol. **69**, 3007–3016
26 Kittlesen, D. J., Chianese-Bullock, K. A., Yao, Z. Q., Braciale, T. J. and Hahn, Y. S. (2000) Interaction between complement receptor gC1qR and hepatitis C virus core protein inhibits T-lymphocyte proliferation. J. Clin. Invest. **106**, 1239–1249
27 Jiang, J., Zhang, Y., Krainer, A. R. and Xu, R. M. (1999) Crystal structure of human p32, a doughnut-shaped acidic mitochondrial matrix protein. Proc. Natl. Acad. Sci. U.S.A. **96**, 3572–3577
28 Jha, B. K., Salunke, D. M. and Datta, K. (2002) Disulfide bond formation through Cys186 facilitates functionally relevant dimerization of trimeric hyaluronan-binding protein 1 (HABP1)/p32/gC1qR. Eur. J. Biochem. **269**, 298–306
29 Jha, B. K., Salunke, D. M. and Datta, K. (2003) Structural flexibility of multifunctional HABP1 may be important for regulating its binding to different ligands. J. Biol. Chem. **278**, 27464–27472
30 Southern, E. M. (1975) Detection of specific sequences among DNA fragments separated by gel electrophoresis. J. Mol. Biol. **98**, 503–517
31 Towbin, H., Staehelin, T. and Gordon, J. (1979) Electrophoretic transfer of proteins from polyacrylamide gels to nitrocellulose sheets: procedure and some applications. Proc. Natl. Acad. Sci. U.S.A. **76**, 4350–4354
32 Bono, P., Rubin, K., Higgins, J. M. and Hynes, R. O. (2001) Layilin, a novel integral membrane protein, is a hyaluronan receptor. Mol. Biol. Cell **12**, 891–900
33 Biederbick, A., Kern, H. F. and Elsasser, H. P. (1995) Monodansylcadaverine (MDC) is a specific *in vivo* marker for autophagic vacuoles. Eur. J. Cell Biol. **66**, 3–14
34 Meenakshi, J., Anupama, Goswami, S. K. and Datta, K. (2003) Constitutive expression of hyaluronan binding protein 1 (HABP1/p32/gC1qR) in normal fibroblast cells perturbs its growth characteristics and induces apoptosis. Biochem. Biophys. Res. Commun. **300**, 686–693
35 Munafo, D. B. and Colombo, M. I. (2001) A novel assay to study autophagy: regulation of autophagosome vacuole size by amino acid deprivation. J. Cell Sci. **114**, 3619–3629
36 Ogier-Denis, E. and Codogno, P. (2003) Autophagy: a barrier or an adaptive response to cancer. Biochim. Biophys. Acta **1603**, 113–128
37 Dunn, Jr, W. A. (1990) Studies on the mechanisms of autophagy: formation of the autophagic vacuole. J. Cell Biol. **110**, 1923–1933
38 Stromhaug, P. E. and Seglen, P. O. (1993) Evidence for acidity of prelysosomal autophagic/endocytic vacuoles (amphisomes). Biochem. J. **291**, 115–121
39 Schwartz, L. M., Schmith, S. W., Jones, M. E. E. and Osborne, B. (1993) Do all programmed cell deaths occur via apoptosis? Proc. Natl. Acad. Sci. U.S.A. **90**, 980–984
40 Hollenbeck, P. J. (1993) Products of endocytosis and autophagy are retrieved from axons by regulated retrograde organelle transport. J. Cell Biol. **121**, 305–315
41 Bursch, W., Ellinger, A., Gerner, C., Frohwein, U. and Schulte-Hermann, R. (2000) Programmed cell death (PCD). Apoptosis, autophagic PCD, or others? Ann. N. Y. Acad. Sci. **926**, 1–12
42 Guenal, I., Risler, Y. and Mignotte, B. (1997) Down-regulation of actin genes precedes microfilament network disruption and actin cleavage during p53-mediated apoptosis. J. Cell Sci. **110**, 489–495
43 Korichneva, I. and Hammerling, U. (1999) F-actin as a functional target for retro-retinoids: a potential role in anhydroretinal-triggered cell death. J. Cell Sci. **112**, 2521–2528

Received 17 February 2004; accepted 3 March 2004
Published as BJ Immediate Publication 8 March 2004, DOI 10.1042/BJ20040264